Snake Robots
From Biology to Nonlinear Control

K. Y. Pettersen [*] **P. Liljebäck** [*,**] **Ø. Stavdahl** [*]
J. T. Gravdahl [*]

[*] *Norwegian University of Science and Technology (NTNU), Dept. of Engineering Cybernetics, NO-7491 Trondheim, Norway (e-mail: {Kristin.Y.Pettersen, Oyvind.Stavdahl, Tommy.Gravdahl}@itk.ntnu.no)*
[**] *SINTEF ICT, Applied Cybernetics, NO-7465 Trondheim, Norway (e-mail: Pal.Liljeback@sintef.no)*

Abstract:
Inspired by the motion of biological snakes, this paper presents an overview of recent results in modelling and control of snake robots. The objective of the research underlying this paper is to contribute to the mathematical foundation of the control theory of snake robots. To this end, the paper presents two mathematical models of planar snake robot dynamics, which are employed to investigate stabilisability and controllability properties of snake robots. Furthermore, averaging theory is used to derive properties of the velocity dynamics of snake robots. Moreover, a straight line path following controller is proposed and cascaded systems theory is employed to prove that the controller $\mathcal{K}$-exponentially stabilizes a snake robot to any desired straight path.

1. INTRODUCTION

Snake robots are robotic mechanisms designed to move like biological snakes. The advantage of such mechanisms is their long and flexible body, which enables them to move and operate in challenging environments where human presence is unwanted or impossible. Future applications of these mechanisms include search and rescue operations, inspection and maintenance in industrial process plants, and subsea operations.

Due to their many degrees of freedom and unique forms of propulsion, snake robots pose many interesting control design challenges. Research on snake robots has been conducted for several decades. For instance, the world's first snake robot was developed in Japan already in 1972 [Hirose, 1993]. There are, however, still many theoretical and practical aspects of snake robot locomotion which have not yet been addressed in the snake robot literature. Current literature is characterised by numerous approaches to modelling and control of these mechanisms, but a unified theoretical foundation of snake robots has not yet been established. The reader is referred to Liljebäck et al. [2012c] for a detailed review of existing literature on snake robots.

In this paper, we present an overview of recent results in modelling and control of snake robots. The goal of our research is to contribute to the mathematical foundation of the control theory of snake robots. To this end, the paper covers the following topics. In Section 2, we present two models of planar snake robot dynamics. The first model is derived directly from first principles, whereas the second model is based on simplifying assumptions which make it less accurate, but more suitable for model-based control design. In Section 3, one of the models of the snake robot is analysed using nonlinear system analysis tools in order to derive controllability and stabilisability properties of snake robot dynamics. The velocity dynamics of snake robots is investigated in Section 4 using averaging theory. Furthermore, Section 5 considers the problem of enabling a snake robot to track a straight path. Finally, Section 6 presents a summary of the paper. For further details on the specific topics treated in the paper, the reader is referred to Liljebäck et al. [2012b].

2. MODELS OF SNAKE ROBOT LOCOMOTION

In this section, we present two models of planar snake robot locomotion. The second model is based on simplifying assumptions which make it less accurate, but more suitable for model-based control design. The material is based on Liljebäck et al. [2011, 2012b].

2.1 A Complex Model of Snake Robot Locomotion

We consider a planar snake robot consisting of N links of length l interconnected by $N-1$ motorized joints. The kinematics of the robot is defined in terms of the symbols illustrated in Fig. 1. All N links have the same mass m and moment of inertia J. The total mass of the robot is therefore Nm. The mass of each link is uniformly distributed so that the link CM (center of mass) is located at its center point. The snake robot moves in the horizontal plane and has $N+2$ degrees of freedom. The position of the CM (center of mass) of the robot is denoted by $\boldsymbol{p} = (p_x, p_y) \in \mathbb{R}^2$. The absolute angle θ_i of link i is expressed with respect to the global x axis with counterclockwise positive direction. As seen in Fig. 1, the relative angle between link i and link $i+1$ (i.e. the angle of joint i) is given by $\phi_i = \theta_i - \theta_{i+1}$.

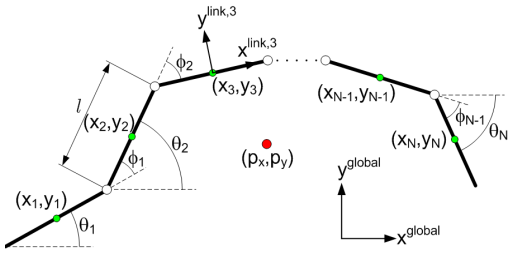

Fig. 1. Kinematic parameters of the snake robot.

Each link is subjected to an anisotropic viscous ground friction force, which means that the ground friction normal to the link is larger than the ground friction parallel to the link. This property is also present in biological snakes and, as will be shown in Section 3, this helps the links glide forward instead of just slipping sideways. Since the friction is anisotropic, a link has two viscous friction coefficients, c_t and c_n, describing the friction force in the tangential and normal direction of the link, respectively.

We define the actuated and unactuated degrees of freedom of the robot as $\boldsymbol{q}_a = [\phi_1, \ldots, \phi_{N-1}]^T \in \mathbb{R}^{N-1}$ and $\boldsymbol{q}_u = [\theta_N, p_x, p_y]^T \in \mathbb{R}^3$, respectively, and we construct the state vector of the robot by defining $\boldsymbol{x}_1 = \boldsymbol{q}_a$, $\boldsymbol{x}_2 = \boldsymbol{q}_u$, $\boldsymbol{x}_3 = \dot{\boldsymbol{q}}_a$, $\boldsymbol{x}_4 = \dot{\boldsymbol{q}}_u$, and $\boldsymbol{x} = \left[\boldsymbol{x}_1^T, \boldsymbol{x}_2^T, \boldsymbol{x}_3^T, \boldsymbol{x}_4^T\right]^T \in \mathbb{R}^{2N+4}$. As shown in Liljebäck et al. [2011], the model can be written as the control-affine system

$$\dot{\boldsymbol{x}} = \begin{bmatrix} \boldsymbol{x}_3 \\ \boldsymbol{x}_4 \\ \overline{\boldsymbol{u}} \\ \mathcal{A}(\boldsymbol{x}) + \mathcal{B}(\boldsymbol{x}_1)\,\overline{\boldsymbol{u}} \end{bmatrix} = \boldsymbol{f}(\boldsymbol{x}) + \sum_{j=1}^{N-1} \left(\boldsymbol{g}_j(\boldsymbol{x}_1)\,\overline{u}_j\right) \quad (1)$$

where

$$\boldsymbol{f}(\boldsymbol{x}) = \begin{bmatrix} \boldsymbol{x}_3 \\ \boldsymbol{x}_4 \\ \boldsymbol{0}_{(N-1)\times 1} \\ \mathcal{A}(\boldsymbol{x}) \end{bmatrix}, \; \boldsymbol{g}_j(\boldsymbol{x}_1) = \begin{bmatrix} \boldsymbol{0}_{(N-1)\times 1} \\ \boldsymbol{0}_{3\times 1} \\ \boldsymbol{e}_j \\ \mathcal{B}_j(\boldsymbol{x}_1) \end{bmatrix} \quad (2)$$

and where $j \in \{1, \ldots, N-1\}$, $\boldsymbol{e}_j$ denotes the jth standard basis vector in $\mathbb{R}^{N-1}$ (the jth column of $\boldsymbol{I}_{N-1}$), $\overline{\boldsymbol{u}} = [\overline{u}_1, \ldots, \overline{u}_{N-1}]^T \in \mathbb{R}^{N-1}$ is a transformed set of control inputs corresponding to the joint accelerations, $\mathcal{A}(\boldsymbol{x}) \in \mathbb{R}^3$ and $\mathcal{B}(\boldsymbol{x}_1) \in \mathbb{R}^{3\times(N-1)}$ are functions of the states, and $\mathcal{B}_j(\boldsymbol{x}_1)$ denotes the jth column of $\mathcal{B}(\boldsymbol{x}_1)$.

2.2 A Simplified Model of Snake Robot Locomotion

Background for the Model The motivation behind the simplified model is to make model-based control design and stability analysis more feasible. The idea behind the model is illustrated in Fig. 2 and is motivated by an analysis presented in Liljebäck et al. [2012b], which shows that:

- The forward motion of a planar snake robot is produced by the link velocity components that are *normal* to the forward direction.
- The change in body shape during forward locomotion primarily consists of relative displacements of the CM of the links *normal* to the forward direction of motion.

Based on these two properties, the simplified model describes the body shape changes of a snake robot as *linear displacements* of the links with respect to each other instead of rotational displacements. The linear displacements occur *normal* to the forward direction of motion and produce friction forces that propel the robot forward. This essentially means that the revolute joints of the snake robot are modelled as prismatic (translational) joints and that the rotational motion of the links during body shape changes is disregarded. However, the model still captures the *effect* of the rotational link motion during body shape changes, which is a linear displacement of the CM of the links normal to the forward direction of motion.

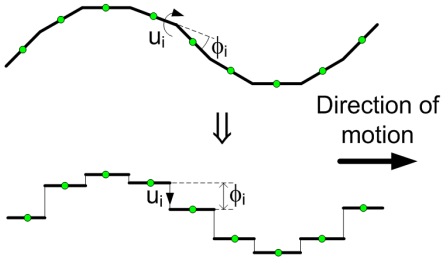

Fig. 2. The idea behind the simplified model is to model the revolute joints as prismatic joints.

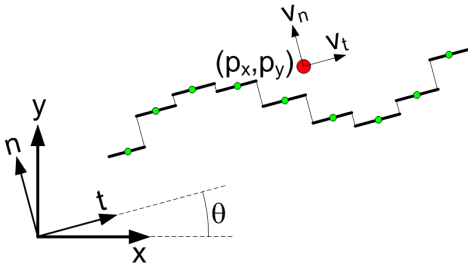

Fig. 3. The robot position and orientation with respect to the two coordinate frames used in the model.

Equations of Motion The snake robot has N links of length l and mass m interconnected by $N-1$ prismatic joints, which control the normal direction distance between the links. The normal direction distance from link i to link $i+1$ is denoted by ϕ_i and represents the coordinate of joint i. The model employs the two coordinate frames illustrated in Fig. 3. The x-y frame is the fixed global frame. The t-n frame is always aligned with the snake robot, i.e. the t and n axis always point in the *tangential* and *normal* direction of the robot, respectively. The global frame orientation of the snake robot, denoted by $\theta \in \mathbb{R}$, is defined as the angle between the t axis and the global x axis with counterclockwise positive direction.

We choose the state vector of the system as

$$\boldsymbol{x} = (\boldsymbol{\phi}, \theta, p_x, p_y, \boldsymbol{v}_\phi, v_\theta, v_t, v_n) \in \mathbb{R}^{2N+4} \quad (3)$$

where $\boldsymbol{\phi} \in \mathbb{R}^{N-1}$ are the joint coordinates, $\theta \in \mathbb{R}$ is the absolute orientation, $(p_x, p_y) \in \mathbb{R}^2$ is the global frame position of the CM, $\boldsymbol{v}_\phi = \dot{\boldsymbol{\phi}} \in \mathbb{R}^{N-1}$ are the joint velocities, $v_\theta = \dot{\theta} \in \mathbb{R}$ is the angular velocity, and $(v_t, v_n) \in \mathbb{R}^2$ is the tangential and normal direction velocity of the snake robot.

Each link is influenced by a ground friction force (acting on the CM of the link) and constraint forces that hold the joints together. A model of these forces is presented in Liljebäck et al. [2012b], where it is also shown that the

complete model of the snake robot can be written as

$$\dot{\boldsymbol{\phi}} = \boldsymbol{v}_\phi \tag{4a}$$
$$\dot{\theta} = v_\theta \tag{4b}$$
$$\dot{p}_x = v_t \cos\theta - v_n \sin\theta \tag{4c}$$
$$\dot{p}_y = v_t \sin\theta + v_n \cos\theta \tag{4d}$$
$$\dot{\boldsymbol{v}}_\phi = \overline{\boldsymbol{u}} \tag{4e}$$
$$\dot{v}_\theta = -\lambda_1 v_\theta + \frac{\lambda_2}{N-1} v_t \overline{\boldsymbol{e}}^T \boldsymbol{\phi} \tag{4f}$$
$$\dot{v}_t = -\frac{c_t}{m} v_t + \frac{2c_p}{Nm} v_n \overline{\boldsymbol{e}}^T \boldsymbol{\phi} - \frac{c_p}{Nm} \boldsymbol{\phi}^T \boldsymbol{A}\overline{\boldsymbol{D}} \boldsymbol{v}_\phi \tag{4g}$$
$$\dot{v}_n = -\frac{c_n}{m} v_n + \frac{2c_p}{Nm} v_t \overline{\boldsymbol{e}}^T \boldsymbol{\phi} \tag{4h}$$

where $\overline{\boldsymbol{u}} \in \mathbb{R}^{N-1}$ is a transformed set of control inputs, $\boldsymbol{A}$, $\boldsymbol{D}$, $\overline{\boldsymbol{D}}$, and $\overline{\boldsymbol{e}}$ are constant matrices, c_t and c_n are the tangential and normal direction friction coefficients of the links, c_p is a particular propulsion coefficient, and λ_1 and λ_2 are positive scalar constants which characterise the rotational motion of the robot.

3. CONTROLLABILITY AND STABILISABILITY ANALYSIS OF SNAKE ROBOTS

In this section, we consider the model in (1) and employ nonlinear system analysis tools for investigating fundamental properties of snake robot dynamics. The material is based on Liljebäck et al. [2011].

3.1 Stabilisability Properties of Planar Snake Robots

We begin by presenting a fundamental theorem concerning the properties of an asymptotically stabilising control law for snake robots to any equilibrium point.

The model in (1) maps the state $\boldsymbol{x}$ and the control input $\overline{\boldsymbol{u}}$ of the robot into the resulting derivative of the state vector, $\dot{\boldsymbol{x}}$. For any equilibrium point ($\boldsymbol{x}_1 = \boldsymbol{x}_1^e$, $\boldsymbol{x}_2 = \boldsymbol{x}_2^e$, $\boldsymbol{x}_3 = \boldsymbol{0}$, $\boldsymbol{x}_4 = \boldsymbol{0}$), where $(\boldsymbol{x}_1^e, \boldsymbol{x}_2^e)$ is the configuration of the system at the equilibrium point, we have that $\dot{\boldsymbol{x}} = \boldsymbol{0}$. A well-known result presented in Brockett [1983] states that a necessary condition for the existence of a *time-invariant* (i.e. not explicitly dependent on time) *continuous* state feedback control law, $\overline{\boldsymbol{u}} = \overline{\boldsymbol{u}}(\boldsymbol{x})$, that makes $(\boldsymbol{x}_1^e, \boldsymbol{x}_2^e, \boldsymbol{0}, \boldsymbol{0})$ asymptotically stable, is that the image of the mapping $(\boldsymbol{x}, \overline{\boldsymbol{u}}) \mapsto \dot{\boldsymbol{x}}$ contains some neighbourhood of $\dot{\boldsymbol{x}} = \boldsymbol{0}$. A result presented in Coron and Rosier [1994] states that a control system that can be asymptotically stabilised (in the Filippov sense) by a *time-invariant discontinuous* state feedback law can be asymptotically stabilised by a *time-varying continuous* state feedback law. If, moreover, the control system is *affine* (i.e. linear with respect to the control input), then it can be asymptotically stabilised by a *time-invariant continuous* state feedback law. These results can be used to prove the following fundamental theorem for planar snake robots:

Theorem 1. An asymptotically stabilising control law for a planar snake robot described by (1) to any equilibrium point must be time-varying, i.e. of the form $\overline{\boldsymbol{u}} = \overline{\boldsymbol{u}}(\boldsymbol{x}, t)$.

3.2 Controllability Analysis of Planar Snake Robots

In this section, we investigate the controllability of planar snake robots described by the model (1).

Controllability with Isotropic Ground Friction We begin by first assuming that the viscous ground friction is isotropic (i.e. not anisotropic as described in Section 2.1). In this case, it turns out that the equations of motion take on a particularly simple form that enables us to study the controllability by inspecting the equations of motion. In particular, we show in Liljebäck et al. [2011] that the CM acceleration of the snake robot can be written as

$$\begin{bmatrix} \ddot{p}_x \\ \ddot{p}_y \end{bmatrix} = -\frac{c}{m} \begin{bmatrix} \dot{p}_x \\ \dot{p}_y \end{bmatrix} \tag{5}$$

which implies that the snake robot is unable to accelerate its CM when it starts from rest. We can therefore state the following theorem:

Theorem 2. A planar snake robot influenced by *isotropic* viscous ground friction is *not controllable*.

Controllability with Anisotropic Ground Friction The equations of motion of the snake robot in (1) become far more complex under anisotropic friction conditions. However, we can still study the controllability of the robot by investigating Lie brackets of the system vector fields, i.e. the drift vector field $\boldsymbol{f}(\boldsymbol{x})$ and the control vector fields $\boldsymbol{g}_j(\boldsymbol{x}_1)$ of the snake robot defined in (1). To calculate Lie brackets, we assume that the snake robot consists of $N = 4$ links, which gives us a $(2N + 4) = 12$-dimensional state space. The following controllability results will also be valid for snake robots with more links since a robot with $N > 4$ links can behave as a robot with $N = 4$ links by fixing $(N - 4)$ joint angles at zero degrees and allowing the remaining three joint angles to move.

Using Lie bracket calculations, we define the *accessibility algebra* [Nijmeijer and Schaft, 1990] of our system, evaluated at an equilibrium point $\boldsymbol{x}^e$, as

$$\begin{aligned} \boldsymbol{\Delta}(\boldsymbol{x}^e) = [\boldsymbol{g}_1, \boldsymbol{g}_2, \boldsymbol{g}_3, [\boldsymbol{f}, \boldsymbol{g}_1], [\boldsymbol{f}, \boldsymbol{g}_2], [\boldsymbol{f}, \boldsymbol{g}_3], \\ [\boldsymbol{f}, [\boldsymbol{f}, \boldsymbol{g}_1]], [\boldsymbol{f}, [\boldsymbol{f}, \boldsymbol{g}_2]], [\boldsymbol{f}, [\boldsymbol{f}, \boldsymbol{g}_3]], \\ [[\boldsymbol{f}, \boldsymbol{g}_1], [\boldsymbol{f}, \boldsymbol{g}_2]], [[\boldsymbol{f}, \boldsymbol{g}_1], [\boldsymbol{f}, \boldsymbol{g}_3]], [[\boldsymbol{f}, \boldsymbol{g}_2], [\boldsymbol{f}, \boldsymbol{g}_3]]] \end{aligned} \tag{6}$$

which we employ in Liljebäck et al. [2011] to prove the following theorem:

Theorem 3. A planar snake robot with $N \geq 4$ links influenced by *anisotropic* viscous ground friction ($c_t \neq c_n$) is *locally strongly accessible* from any equilibrium point $\boldsymbol{x}^e$ except for certain singular configurations.

Accessibility does *not* imply controllability since it only infers conclusions on the dimension of the reachable space from an equilibrium point. The singular configurations referred to in Theorem 3 mean that the dimension of the reachable space from certain configurations is not full-dimensional, as revealed by the following property:

Property 4. The accessibility algebra $\boldsymbol{\Delta}(\boldsymbol{x}^e)$ drops rank at equilibrium points where all relative joint angles are equal ($\phi_1 = \ldots = \phi_{N-1}$).

Property 4 is interesting since it suggests that the joint angles of a snake robot should be *out of phase* during snake locomotion. This agrees well with observations of biological snake locomotion, which generally consists of oscillatory motion patterns that are propagated along the body of the snake.

The next theorem can be shown to hold by investigating so-called *good* and *bad* Lie brackets of the system using

sufficient conditions presented in Sussmann [1987], Bianchini and Stefani [1990].

Theorem 5. At any equilibrium point $\boldsymbol{x}^e$, a planar snake robot with $N \geq 4$ links influenced by viscous ground friction does *not* satisfy sufficient conditions for *small-time local controllability* (STLC).

STLC implies that the control input can steer the system in any direction in an arbitrarily small amount of time. Theorem 5 does not claim that a snake robot is *not* STLC since the theorem only considers sufficient conditions. Note also that STLC is not a requirement for controllability since it is in fact a stronger property than controllability. In summary, the above results do not enable us to conclude that a snake robot influenced by anisotropic ground friction is controllable. However, the above results are hopefully an important step towards formally proving that such mechanisms are controllable, which we consider highly likely to be the case.

4. AVERAGING ANALYSIS OF SNAKE ROBOT LOCOMOTION

In this section, we use *averaging theory* [Sanders et al., 2007] to derive properties of the velocity dynamics of a snake robot during *lateral undulation* [Hirose, 1993], which is the most common type of snake locomotion. The material is based on Liljebäck et al. [2012b]

4.1 An Averaged Model of the Velocity Dynamics

We begin by using the simplified model in (4) to derive a model which describes the *average* effect of the oscillatory joint motion on the propulsion of the robot. The gait pattern lateral undulation is achieved by controlling joint $i \in \{1, \ldots, N-1\}$ according to

$$\phi_{i,\text{ref}} = \alpha \sin\left(\omega t + (i-1)\,\delta\right) + \phi_o \tag{7}$$

where α and ω are the amplitude and frequency, respectively, of the sinusoidal joint motion, δ determines the phase shift between the joints, ϕ_o is a joint offset assumed in this section to be constant, and where

$$\dot{\phi}_{i,\text{ref}} = \alpha\omega \cos\left(\omega t + (i-1)\,\delta\right) \tag{8}$$

During lateral undulation, where the snake robot joints move according to (7) and (8), it can be shown that the velocity dynamics of the simplified model, which is given by (4f), (4g), and (4h), can be rewritten as

$$\frac{\mathrm{d}\boldsymbol{v}}{\mathrm{d}\tau} = \varepsilon \boldsymbol{f}(\tau, \boldsymbol{v}) \tag{9}$$

where $\boldsymbol{v} = [v_t, v_n, v_\theta]^T \in \mathbb{R}^3$ is the velocity state vector, $\boldsymbol{f}(t, \boldsymbol{v})$ is a nonlinear vector function, $\tau = \omega t$ is the time variable scaled by the frequency of the sinusoidal joint motion, and $\varepsilon = 1/\omega$ is a parameter characterising the periodic perturbations of the system. The model in (9) is in the standard form of averaging [Sanders et al., 2007], which means that a system that, in 'average', behaves similarly to the system in (9) is given by

$$\frac{\mathrm{d}\boldsymbol{v}}{\mathrm{d}\tau} = \varepsilon \frac{1}{2\pi} \int_0^{2\pi} \boldsymbol{f}(\tau, \boldsymbol{v}) \mathrm{d}\tau \tag{10}$$

We show in Liljebäck et al. [2012b] that the resulting averaged model is given by the linear system

$$\dot{\boldsymbol{v}} = \mathcal{A}\left(\phi_o\right) \boldsymbol{v} + \boldsymbol{b}\left(\alpha, \omega, \delta\right) \tag{11}$$

where

$$\mathcal{A}\left(\phi_o\right) = \begin{bmatrix} -\dfrac{c_t}{m} & \dfrac{2\left(N-1\right)}{Nm} c_p \phi_o & 0 \\ \dfrac{2\left(N-1\right)}{Nm} c_p \phi_o & -\dfrac{c_n}{m} & 0 \\ \lambda_2 \phi_o & 0 & -\lambda_1 \end{bmatrix} \tag{12}$$

$$\boldsymbol{b}\left(\alpha, \omega, \delta\right) = \begin{bmatrix} \dfrac{c_p}{2Nm} \alpha^2 \omega k_\delta \\ 0 \\ 0 \end{bmatrix} \tag{13}$$

and where k_δ is a function of the constant phase shift, δ.

4.2 Properties of the Forward Velocity

Since the averaged model in (11) is a linear system, we can easily show that the average velocity of the snake robot will converge exponentially to the steady state velocity

$$\boldsymbol{v}^* = \begin{bmatrix} v_t^* \\ v_n^* \\ v_\theta^* \end{bmatrix} = -\mathcal{A}^{-1}\boldsymbol{b}, \tag{14}$$

where the analytical expression for the steady state forward velocity is given by

$$v_t^* = \alpha^2 \omega k_\delta \frac{N c_n c_p}{2\left(N^2 c_t c_n - \left(4N^2 - 8N + 4\right) c_p^2 \phi_o^2\right)} \tag{15}$$

The result in (15) is interesting since it enables us to derive some fundamental relationships between the gait pattern parameters and the forward velocity of the snake robot. In particular, we see from (15) that the forward velocity is proportional to the term $\alpha^2 \omega k_\delta$, which means that the following theorem holds:

Theorem 6. Consider a planar snake robot with N links modelled by (4) and moving according to the gait pattern lateral undulation defined in (7) and (8). The average forward velocity of the snake robot will converge exponentially to a value which is proportional to:
- the squared amplitude of the sinusoidal joint motion, α^2.
- the angular frequency of the sinusoidal joint motion, ω.
- the function of the constant phase shift, δ, given by k_δ.

Moreover, for a given α and ω, the phase shift, δ, that maximises the average forward velocity is given by the δ that maximises k_δ.

5. PATH FOLLOWING CONTROL

In this section, we consider the problem of enabling a snake robot to track a straight path. The material is based on Liljebäck et al. [2012a].

Remark 7. The control design in this section is based on the simplified model in (4). In Liljebäck et al. [2011], the authors employ the more complex model in (1) to analyse a path following controller using a Poincaré map.

5.1 The Control Objective

The control objective is to steer the snake robot so that it converges to and subsequently tracks a straight path while maintaining a heading which is parallel to the path. To this end, we define the global coordinate system (see Fig. 3) so that the global x axis is aligned with the desired straight path. The y axis position, p_y, is thereby the cross-track error and the orientation, θ, is the angle that the robot

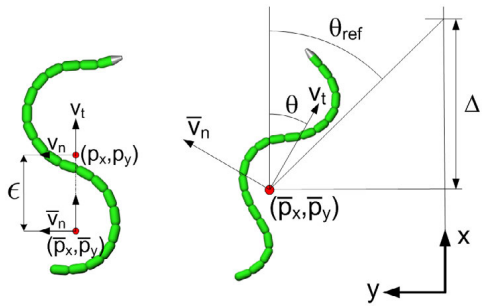

Fig. 4. Left: The coordinate transformation of the snake robot. Right: The Line-of-Sight (LOS) guidance law.

forms with the desired path. The control objective is thus to design a feedback control law such that

$$\lim_{t\to\infty} \; p_y(t) = 0 \tag{16}$$

$$\lim_{t\to\infty} \; \theta(t) = 0 \tag{17}$$

We choose not to explicitly control the forward velocity. Instead, the forward velocity is assumed to be a non-zero and positive parameter satisfying $v_t \in [V_{\min}, V_{\max}]$, where $V_{\min}$ and $V_{\max}$ are boundary values.

5.2 Model Transformation

To simplify the control design, we introduce the change of coordinates illustrated to the left in Fig. 4. In particular, we move the point that determines the position of the snake robot a specific distance along the tangential direction of the robot to a new location $(\overline{p}_x, \overline{p}_y)$, which is precisely where the body shape changes of the robot (characterised by $\overline{\boldsymbol{e}}^T\boldsymbol{\phi}$ in (4h)) generate a pure rotational motion and no sideways force. With this coordinate transformation, the model of the robot is transformed into

$$\dot{\boldsymbol{\phi}} = \boldsymbol{v}_\phi \tag{18a}$$

$$\dot{\theta} = v_\theta \tag{18b}$$

$$\dot{\overline{p}}_y = v_t \sin\theta + \overline{v}_n \cos\theta \tag{18c}$$

$$\dot{\boldsymbol{v}}_\phi = \overline{\boldsymbol{u}} \tag{18d}$$

$$\dot{v}_\theta = -\lambda_1 v_\theta + \frac{\lambda_2}{N-1} v_t \overline{\boldsymbol{e}}^T \boldsymbol{\phi} \tag{18e}$$

$$\dot{\overline{v}}_n = X v_\theta + Y \overline{v}_n \tag{18f}$$

where $\overline{v}_n$ is the transformed sideways velocity and where X and Y are two scalar constants.

5.3 The Path Following Controller

We control the snake robot according to the gait pattern lateral undulation defined in (7) and we make the joints track these reference signals by specifying the control input according to the exponentially stabilizing control law

$$\overline{\boldsymbol{u}} = \ddot{\boldsymbol{\phi}}_{\text{ref}} + k_{v_\phi}\left(\dot{\boldsymbol{\phi}}_{\text{ref}} - \dot{\boldsymbol{\phi}}\right) + k_\phi\left(\boldsymbol{\phi}_{\text{ref}} - \boldsymbol{\phi}\right) \tag{19}$$

where $k_\phi > 0$ and $k_{v_\phi} > 0$ are scalar controller gains and $\boldsymbol{\phi}_{\text{ref}} \in \mathbb{R}^{N-1}$ is the reference defined in (7).

In order to steer the robot towards the desired path, we employ the Line-of-Sight (LOS) guidance law

$$\theta_{\text{ref}} = -\arctan\left(\frac{\overline{p}_y}{\Delta}\right) \tag{20}$$

where $\overline{p}_y$ is the cross-track error and $\Delta > 0$ is a design parameter referred to as the *look-ahead distance*. As illustrated to the right in Fig. 4, the LOS angle θ_{ref} corresponds to the orientation of the snake robot when it is headed towards the point located a distance Δ ahead of the snake robot along the desired path. We use the joint offset coordinate ϕ_o in (7) to ensure that the heading of the snake robot θ tracks the LOS angle given by (20). In particular, we show in Liljebäck et al. [2012a] that choosing ϕ_o as

$$\begin{aligned}\phi_o = \frac{1}{\lambda_2 v_t}\Big(&\ddot{\theta}_{\text{ref}} + \lambda_1\dot{\theta}_{\text{ref}} - k_\theta(\theta - \theta_{\text{ref}}) \\ &- \frac{\lambda_2}{N-1} v_t \sum_{i=1}^{N-1} \alpha \sin(\omega t + (i-1)\,\delta)\Big)\end{aligned} \tag{21}$$

where $k_\theta > 0$ is a scalar controller gain, enables us to combine the model and the controller of the snake robot into a cascaded system of the form

$$\begin{bmatrix}\dot{\overline{p}}_y \\ \dot{\overline{v}}_n\end{bmatrix} = \boldsymbol{C}(\overline{p}_y)\begin{bmatrix}\overline{p}_y \\ \overline{v}_n\end{bmatrix} + \boldsymbol{H}_\xi(\overline{p}_y, \overline{v}_n, \boldsymbol{\xi})\boldsymbol{\xi} \tag{22a}$$

$$\dot{\boldsymbol{\xi}} = \begin{bmatrix}0 & 1 \\ -k_\theta & -\lambda_1\end{bmatrix}\boldsymbol{\xi} + \boldsymbol{H}_\eta\boldsymbol{\eta} \tag{22b}$$

$$\dot{\boldsymbol{\eta}} = \begin{bmatrix}\boldsymbol{0}_{(N-1)\times(N-1)} & \boldsymbol{I}_{N-1} \\ -k_\phi\boldsymbol{I}_{N-1} & -k_{v_\phi}\boldsymbol{I}_{N-1}\end{bmatrix}\boldsymbol{\eta} \tag{22c}$$

where $\boldsymbol{\eta}$ is the error variable of the joint coordinates, $\boldsymbol{\xi}$ is the error variable of the heading, and where $\boldsymbol{C}(\overline{p}_y)$, $\boldsymbol{H}_\xi$, and $\boldsymbol{H}_\eta$ are state-dependent matrices. The model in (22) is a cascaded system since the $\boldsymbol{\eta}$-dynamics perturbs the $\boldsymbol{\xi}$-dynamics through the interconnection term $\boldsymbol{H}_\eta\boldsymbol{\eta}$, and the $\boldsymbol{\xi}$-dynamics perturbs the $(\overline{p}_y, \overline{v}_n)$-dynamics through the interconnection term $\boldsymbol{H}_\xi(\overline{p}_y, \overline{v}_n, \boldsymbol{\xi})\boldsymbol{\xi}$. We show in Liljebäck et al. [2012a] that the cascaded system is $\mathcal{K}$-exponentially stable and that the following theorem holds:

Theorem 8. Consider a planar snake robot described by the model (18). If the look-ahead distance Δ of the LOS guidance law (20) is chosen such that

$$\Delta > \frac{|X|}{|Y|}\left(1 + \frac{V_{\max}}{V_{\min}}\right) \tag{23}$$

then the path following controller defined by (7), (19), (20), and (21) guarantees that the control objectives (16) and (17) are achieved for any set of initial conditions satisfying $v_t \in [V_{\min}, V_{\max}]$.

5.4 Simulation Results

To illustrate the performance of the straight line path following controller, we present in Fig. 5 a simulation result (generated using Matlab) where a snake robot described by the simplified model in (4) with $N = 10$ links is controlled according to the control law proposed in Section 5.3. The robot, which is initially headed away from the desired straight path, converges rapidly towards the path as predicted. See Liljebäck et al. [2012a] for more details regarding these simulation results.

5.5 Experimental Results

We have also investigated the performance of the proposed path following controller using one of our physical snake robots, *Wheeko*. One of the experimental results is shown

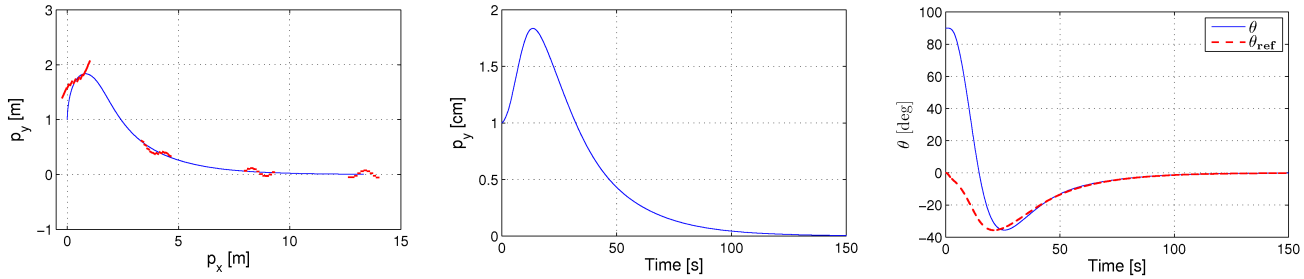

(a) The path of the snake robot. (b) Cross-track error, p_y. (c) Heading angle, θ.

Fig. 5. Simulation of the proposed straight line path following controller.

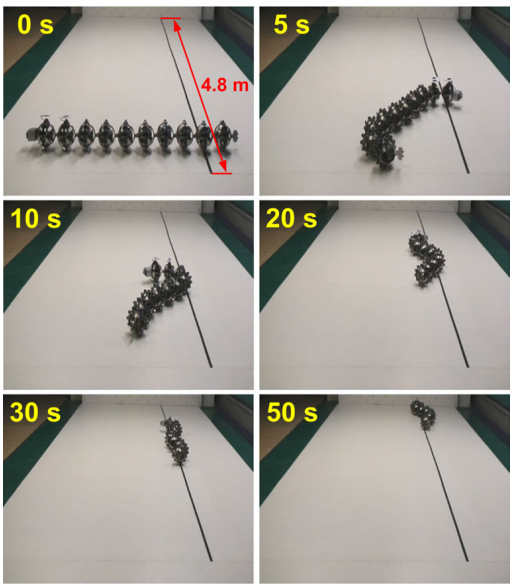

Fig. 6. Experimental investigation of the proposed straight line path following controller.

in Fig. 6. The robot is initially headed away from the desired path, which is indicated by a black line on the floor. The robot converges rapidly to the path and continues to locomote along the path. See Liljebäck et al. [2012a] for more details regarding these experimental result.

6. SUMMARY AND FUTURE WORK

Inspired by the motion of biological snakes, the objective of the research underlying this paper has been to increase our understanding of snake robot locomotion through analytical investigations of equations of motion. The paper has presented two mathematical models of planar snake robot dynamics, which were employed to investigate stabilisability and controllability properties of snake robots. Averaging theory was used to derive properties of the velocity dynamics of snake robots conducting lateral undulation. Furthermore, a straight line path following controller was proposed and cascaded systems theory was employed to prove that the controller $\mathcal{K}$-exponentially stabilizes a snake robot to any desired straight path.

Many research challenges still remain before we will see useful applications of snake robots, and much remains to be understood about the dynamics of these fascinating mechanisms. An important topic which the authors are currently investigating concerns new models and control strategies to support intelligent and adaptive snake robot locomotion in challenging and cluttered environments, i.e. environments which are not flat.

REFERENCES

R. M. Bianchini and G. Stefani. Graded approximations and controllability along a trajectory. *SIAM J. Control and Optimization*, 28(4):903–924, 1990.

R. Brockett. Asymptotic stability and feedback stabilization. *Differential Geometric Control Theory*, pages 181–191, 1983.

J.-M. Coron and L. Rosier. A relation between continuous time-varying and discontinuous feedback stabilization. *J. of Mathematical Systems, Estimation, and Control*, 4 (1):67–84, 1994.

S. Hirose. *Biologically Inspired Robots: Snake-Like Locomotors and Manipulators*. Oxford University Press, Oxford, 1993.

P. Liljebäck, K. Y. Pettersen, Ø. Stavdahl, and J. T. Gravdahl. Controllability and stability analysis of planar snake robot locomotion. *IEEE Trans. Automatic Control*, 56(6):1365–1380, 2011.

P. Liljebäck, I. U. Haugstuen, and K. Y. Pettersen. Path following control of planar snake robots using a cascaded approach. *IEEE Trans. Control Systems Technology*, 20 (1):111–126, 2012a.

P. Liljebäck, K. Y. Pettersen, Ø. Stavdahl, and J. T. Gravdahl. *Snake Robots - Modelling, Mechatronics, and Control*. Advances in Industrial Control. Springer, 2012b.

P. Liljebäck, K. Y. Pettersen, Ø. Stavdahl, and J. T. Gravdahl. A review on modelling, implementation, and control of snake robots. *Robotics and Autonomous Systems*, 60(1):29–40, 2012c.

Henk Nijmeijer and A. van der Schaft. *Nonlinear Dynamical Control Systems*. Springer-Verlag, New York, 1990.

J. A. Sanders, F. Verhulst, and J. Murdock. *Averaging Methods in Nonlinear Dynamical Systems*, volume 59 of *Applied Mathematical Sciences*. Springer, 2nd edition, 2007.

H. J. Sussmann. A general theorem on local controllability. *SIAM Journal on Control and Optimization*, 25(1):158–194, 1987. ISSN 0363-0129.